Desalination and Water Treatment
www.deswater.com

doi:10.5004/dwt.2018.22743

124 (2018) 160–176
August

Deactivation and regeneration of photocatalysts: a review

Xiaoju Yan[a], Yu Tang[a], Cong Ma[b,c,*], Ying Liu[b], Jun Xu[d]

[a]*College of Hydrology and Water Resources, Hohai University, Nanjing, 210024, China. Tel. +86 13912993906, email: wshyxj@126.com (X.J. Yan), Tel. 15950506895, email: ytang_hhu@163.com (Y. Tang)*
[b]*State Key Laboratory of Separation Membranes and Membrane Processes, School of Environmental and Chemical Engineering, Tianjin Polytechnic University, Tianjin, 300387, China. Tel. +86 15122382805, email: macong_0805@126.com (C. Ma), Tel. +86 13642117368, email: ly9423@163.com (Y. Liu)*
[c]*Department of Chemical and Biomolecular Engineering, University of Connecticut, 191 Auditorium Rd. Unit 3222, Storrs, CT 06269-3222, United States*
[d]*Department of Civil Engineering and Architecture, Nanyang Normal University, Nanyang, 473061, China. Tel. +86 18749043725, email: xujunhit@126.com (J. Xu)*

Received 30 November 2017; Accepted 9 July 2018

ABSTRACT

Heterogeneous photocatalysis is considered a suitable approach for decontamining and mineralizing organic pollutants because of its high efficiency, low energy consumption, and satisfactory environmental compatibility. However, photocatalyst deactivation has been pointed out as a key disadvantage that hinders practical applications. This paper provides a literature review on deactivation and regeneration of photocatalysts, with aspects such as lifetime, deactivation mechanism, and regeneration efficiency/characterization of deactivated photocatalysts being comprehensively studied. We believe this work can help better understand the deactivation and regeneration processes of photocatalysts, which is necessary to prolong the lifetime of these materials and to further improve the practical application of photocatalysis.

Keywords: Photocatalysis; Photocatalyst; Deactivation; Regeneration; Lifetime

1. Introduction

Advanced oxidation processes (AOPs) such as UV/H_2O_2 [1–5], ozonation [6–10], Fenton [11–15], sonolysis [16–20], and photocatalysis [21–25] have been widely explored to mitigate a large variety of pollutants present in various environmental media. As one of the novel AOPs, heterogeneous photocatalytic oxidation was developed in the 1970s and acquires special interest when solar light is used. When photo energy is greater than or equal to the band gap energy of photocatalysts, the electron will be photoexcited to the empty conduction band in femtoseconds, meanwhile creating the electron-hole pair. After series of chain reactions, powerful active oxidants of hydroxyls formed, which is capable of decomposing almost all types of organic contaminants. Photocatalysis finds applications in air purification and wastewater treatment, although it suffers from photocatalyst deactivation as the reaction proceeds. By applying photocatalyst on polluted air, the strong adsorption of products or intermediates on the photocatalyst surface hindered the photocatalytic activity of the photocatalyst. When treating wastewater, deactivation mechanism is more complex considering the complicacy of effluent. From the economical point of view, photocatalyst deactivation represents a major drawback hindering industrial applications. Recently, significant effort has been devoted to clarify the origin of photocatalyst deactivation and overcome this issue. Some aspects related to photocatalyst deactivation and regeneration need to be emphasized: (i) determining photocatalyst deactivation, (ii) deactivation reasons other than strong surface adsorption of some intermediates and products, (iii) selection of a suitable regeneration methods, and (iv) methods solving or mitigating photocatalyst deactivation other than regeneration.

*Corresponding author.

This paper provides a critical review on recent research studies dealing with deactivation and regeneration of photocatalyst. In particular, this review focuses on the following aspects: quantification of photocatalyst lifetime, photocatalyst deactivation mechanisms, regeneration of deactivated photocatalysts, additional anti-deactivation approaches, and characterization of deactivated/regenerated photocatalysts. Certain classification has been applied in terms of different research field (air or wastewater treatment) if possible in the main text. We believe that a better understanding of these aspects is helpful in further expanding the practical applications of photocatalysis.

2. Summary of experimental conditions

According to the photocatalysts in liquid or gaseous media, the main experimental conditions (e.g., target contaminant, photocatalyst, light source, and photoreactor used) in published studies dealing with photocatalyst deactivation and regeneration are separately listed in Tables 1 and 2.

2.1. Target contaminant

The main gaseous target contaminants include toluene, NO, H_2S, acetylene, and cyclohexane, while the main liquid target contaminants studied have been organic dyes, wastewater, phenol, Cr(VI), and phthalic acid. Despite the large number of contaminants studied, published works mostly focused on the single removal of various compounds in the laboratory under idealized conditions [31]. Recently, target contaminants from real wastewater or ambient air were used to study photocatalyst deactivation under more realistic practical engineered treatment operations. Moreover, compared with single compounds under laboratory conditions, real wastewater and ambient air samples contain numerous components that can complicate the deactivation process.

Carbonaro et al. [45] monitored the degradation of four pharmaceutical micropollutants (i.e., iopromide, acetaminophen, sulfamethoxazole, and carbamazepine) from both a pH-buffered electrolyte solution and a biologically treated wastewater effluent (WWE) with the aim to study the effects

Table 1
Experimental conditions of published studies dealing with photocatalyst deactivation and regeneration in gaseous phase

Year	Target contaminant	Photocatalyst (self-made/commercial)		Light source (UV/VL)		Photoreactor (batch flow/ continuous flow)	Ref.
2003	Octamethyltrisiloxane	TiO_2 thin films	Self-made	Black light bulbs	UV	Batch flow	[26]
2003	Diethyl sulfide	UV-100 TiO_2 deposited onto the internal surface of a Pyrex coil	Self-made	Six 8W UV	UV	Continuous flow	[27]
2004	n-C_7H_{16}, SO_2	ZnO, TiO_2	Self-made	400W high pressure mercury lamp (365 nm)	UV	Batch flow	[28]
2008	Toluene	TiSn, TiZr, TiO_2/SnO_2, TiO_2/ZrO_2	Self-made	Four 6W UV (356 nm)	UV	Continuous flow	[29]
2008	H_2S	TiO_2/M-MCM-41 (M = Cr or Ce)	Self-made	OSRAM L8W/954 (460, 540 and 615 nm);PHILIPS TL8W/05 FAM (365 nm)	UV/VL	Continuous flow	[30]
2010	Ambient office air in two office building	Degussa P25, 3wt% WO_3 coated on Degussa P25	Commercial/ Self-made	Philips TUV 16W T5 4P-SE	UV	Continuous flow	[31]
2011	NO	Pt/TiO_2	Self-made	15 W low pressure mercury lamp(365 nm)	UV	Batch flow	[32]
2011	Toluene methylcyclohexane	TiO_2-ZnO thin film	Self-made	Four 4 W Black light lamps	UV	Continuous flow	[33]
2011	Cyclohexane	MoOx/TiO_2	Self-made	40 W fluorescent lamp (365 nm)	UV	Continuous flow	[34]
2012	H_2S	TiO_2 was loaded on the support.	Self-made	8 W (185 nm, 254 nm, 365 nm)	UV	Continuous flow	[35]
2013	Toluene	TiO_2 P25	Commercial	4 W UV (365 nm)	UV	Continuous flow	[36]
2014	Acetylene	P25 Degussa TiO_2 nanoparticles deposited on glass fibres	Self-made	Two 24 W Philips UV lamps (365 nm).	UV	Continuous flow	[37]
2015	NO	TiO_2-rGO	Self-made	35 W incandescent lamp from Philips Company	VL	Continuous flow	[38]

Table 2
Experimental conditions of published studies dealing with photocatalyst deactivation and regeneration in liquid phase

Year	Target contaminant	Photocatalyst (self-made/commercial)		Light source (UV/VL)		Photoreactor (batch flow/ continuous flow)	Ref.
2005	Cr(VI)	TiO_2	Self-made	125W (300–400 nm)	UV	Batch flow	[39]
2006	Phenol	TiO_2-anatase thin films were deposited on a fiberglass	Self-made	15 W low pressure mercury lamps	UV	Batch flow	[40]
2009	Dyes	CdS/HMS-PDDA	Self-made	Xenon lamp 120 W (>420 nm)	VL	Batch flow	[41]
2010	Cyclohexane	HombikatUV 100, Hombikat was calcined at 600°C, Solaronix nanopowder is designed for coatings(S450)	Commercial/ Self-made	50 W high pressure mercurylamp (275 nm–388 nm)	UV	Continuous flow	[42]
2010	Organic dye	WACS-200 NMP-200	Self-made	A Spectrolineblack light lamp (365 nm and 182 W) and a 150 W halogen lamp	UV/ VL	Batch flow	[43]
2012	Phthalic acid	TiO_2 P25	Commercial	120 W high pressure mercury lamp	UV	Batch flow	[44]
2013	Wastewater effluent	TiO_2 thin films	Self-made	15W UV-A (365 nm)	UV	Continuous flow	[45]
2014	Waste water	TiO_2/LECA	Self-made	Natural solar light	VL	Batch flow	[46]
2014	15 selected emerging contaminants in water	TiO_2 immobilized on glass spheres	Self-made	2.2 kW Xenon arc lamp	VL	Batch flow	[47]
2016	Methyl orange	TiO_2 P25	Commercial	12 W lamps (254 nm)	UV	Continuous flow	[48]

of non-target constituents present in theWWE matrix. The reactor performance remained stable for over 7d when treating micropollutants in the buffered electrolyte. When the reactor influent was switched to WWE, the treatment efficiencies decreased to varying degrees. A large fraction of the initial catalytic activity was recovered upon switching back to the buffered electrolyte influent after 4 d. However, a fraction of the activity was not recovered, thereby revealing that both the effluent organic matter and the inorganic constituents in the WWE contributed to the observed photocatalyst deactivation. These results demonstrated the marked influence of non-target constituents present in complex matrices on the long-term photocatalyst activity. In addition, these results highlighted the need for further study on this important issue with the aim to advance the development of practical photocatalytic water treatment technologies.

Hay et al. [31] carried out field tests by prototype reactors in two office building locations in CT, USA with the aim to investigate photocatalyst deactivation by silicon-containing volatile and semi-volatile organic compounds (VOCs and SVOCs, respectively) and to in situ determine the durability of the photocatalyst in an office environment. A rapid catalyst deactivation was observed in photocatalytic air purifiers deployed in ambient office air. This deactivation is complex since it likely involves multiple mechanisms and requires further study.

Hence, photocatalyst deactivation under real wastewater or ambient air practical treatment conditions requires further study.

2.2. Photocatalysts

In the photocatalyst research, there are commercial photocatalysts (e.g. Degussa P25 and Hombikat UV 100) and self-made photocatalysts. Most self-made photocatalysts are investigated in order to enhance photocatalytic activity and efficiency, the photostability and anti-photocorrosion [49–53]. Nevertheless,the main factors influencing photocatalyst lifetime require further study.

2.3. Light sources

The number of studies dealing with photocatalyst deactivation and regeneration under visible light (VL) is increasing. Xenon, incandescent, and halogen lamps have been used as solar light simulators and visible light source. Shavisi et al. [46] used natural solar light to degrade ammonia in petrochemical wastewater.

Photocatalysts are typically doped with the aim to make them active towards visible light. Therefore, the deactivation and regeneration mechanisms of photocatalysts under UV light are different than those of doped photocatalysts under visible light conditions. Portela et al. [30] reported Cr^{6+}/Cr^{5+} as the only photospecies susceptible to absorb visible wavelength photons. However, Cr^{6+} was reduced to Cr^{3+} as a result of the photocatalytic process, thereby increasing the concentration of Cr^{3+} and contributing to the deactivation of the catalyst. Kaewgun and Lee [43] reported on a failed regeneration of a NMP-200 catalyst, and this was

tentatively ascribed to the removal of some of the nitrogen species responsible for visible light activation and to the decrease in the surface area produced by the high regeneration temperature.

2.4. Photoreactor

Batch or continuous-flow photoreactors have been used to study the deactivation of photocatalysts. Compared to batch photoreactors, continuous-flow reactors can better simulate real treatment systems and are therefore preferred to study photocatalyst stability, inhibition, and deactivation [37]. Among all the continuous flow reactors, the hard-core photocatalytic reactor equipped with built-in light source manufactured by W.-W Yang has shown the potential application. From Fig. 1 [38], we can see the reactor is connected with flue gas analyzer, making it convenient to evaluate NO removal. Continuous-flow photoreactors are typically based on immobilized photocatalyst systems in which the catalyst particles are deposited on substrates such as glass fibers (Fig. 2) [37], foam nickel catalyst support (Fig. 3) [35], and pyrex coil (Fig. 4) [27].

Photocatalytic membrane reactors (PMRs) combining photocatalysis with membrane filtration represent a promising approach for separating and reusing suspended photocatalysts. These reactors open the possibility for

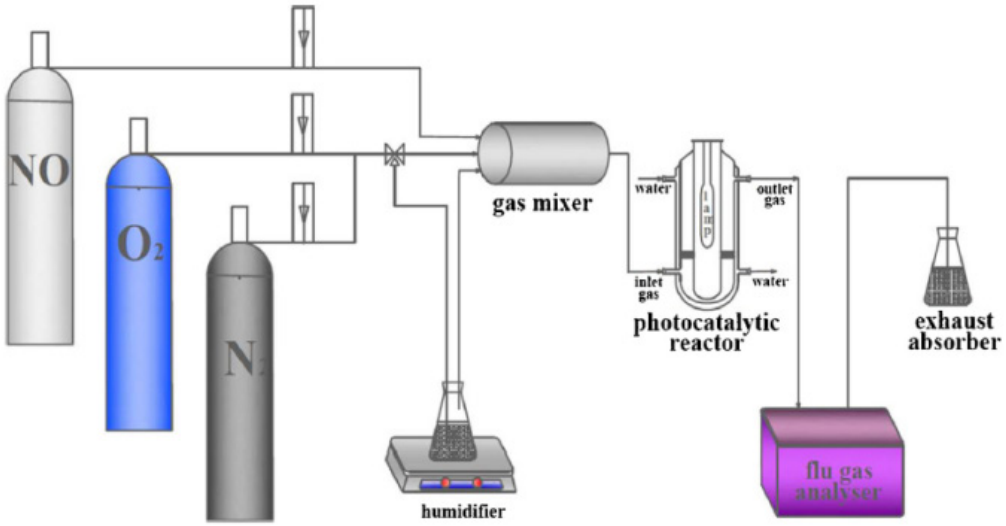

Fig. 1. Schematic diagram of experimental apparatus for photocatalytic activity evaluation [38].

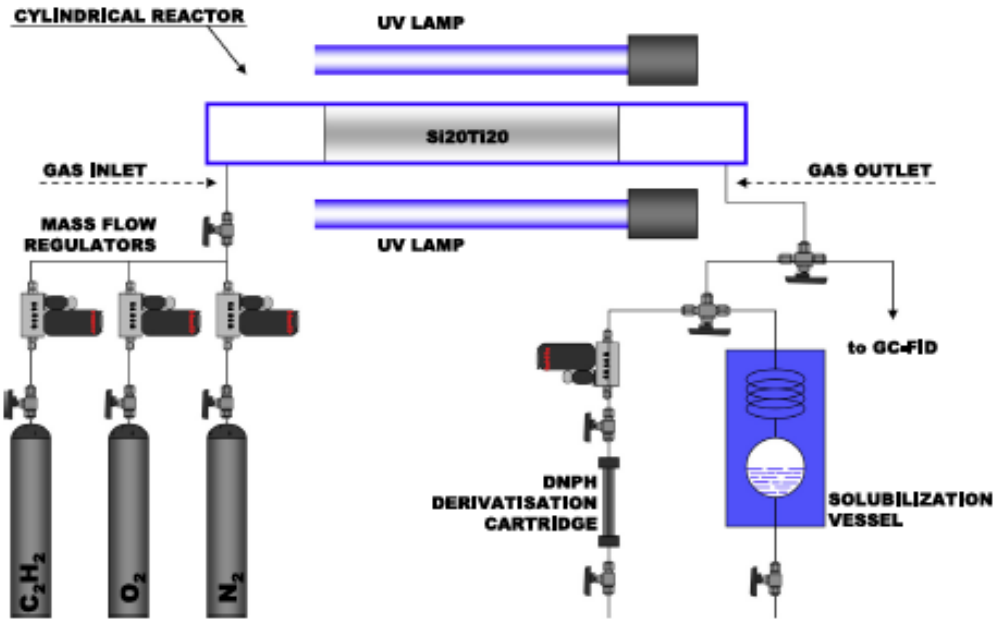

Fig. 2. The scheme of photocatalyst system using glass fibers as support [37].

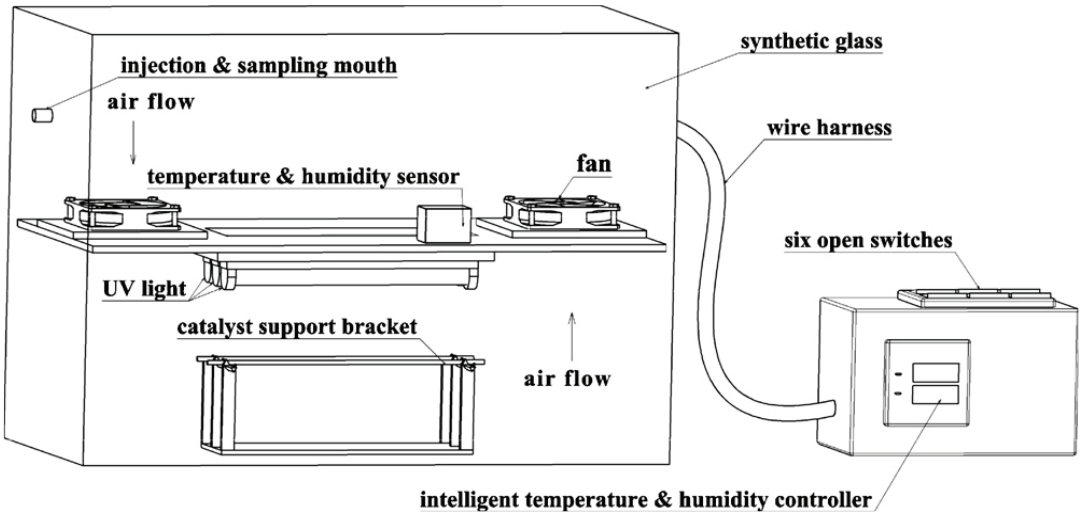

Fig. 3. The scheme of photocatalyst system using foam nickel catalyst as support [35].

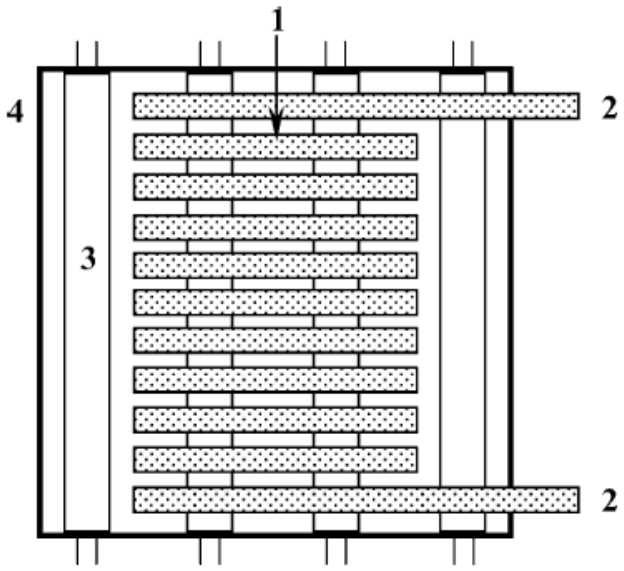

Fig. 4. The scheme of photocatalyst system using pyrex coil as support. (1) Pyrex coil with TiO_2 deposited on the inner side; (2) coil inlet and outlet; (3) ultraviolet lamps; (4) housing with attached aluminum foil [27].

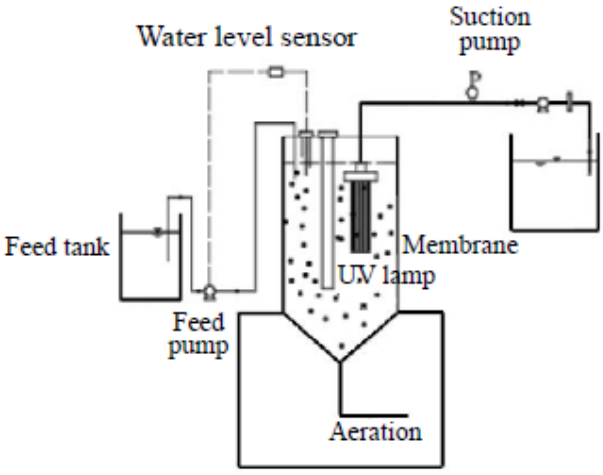

Fig. 5. The general scheme of PMR setup [48].

performing continuous-flow photocatalysis degradation, and can be used to study deactivation and regeneration of photocatalysts. As shown in Fig. 5, Yan et al. [48] designed a new PMR with the UV lamp and the hollow-fiber MF membrane unit placed at the center of the PMR tank and continuous aeration provided by an air diffuser placed at the bottom of the tank. The reactor helped to perform continuous-flow experiment and collect spent photocatalysts for degradation analysis.

Based on the experimental conditions, a summarized conclusion could be drawn: the deactivation mechanism is more complex by adopting the real waste water or ambient air as the target pollutants. Recently, the steady of the self-made photocatalyst are focused on. The main effecting factors on photocatalyst lifetime are still required further study. The mechanism and the experimental methods under the visible light are different than those under the UV light. The continuous photo-reactor with the catalyst support such as the glass fiber, is convenient to the deactivation mechanism. However, the detached troubles could not be ignored either. PMR could be an alternative continuous photo-reactor, because the membrane could intercept the powder photocatalyst in PMR.

3. Quantification of photocatalyst lifetime

The deactivation of photocatalysts and the quantification their lifetime are reviewed in Table 3. Photocatalyst deactivation is calculated as by dividing the target contaminant concentration after and before degradation (C_{out}/C_{in}) or by determining the conversion rate for a target contaminant concentration. Yang et al. [41] reported a C/C_0 of

Table 3
Summary of photocatalyst lifetime quantification

Target contaminant	Photocatalyst	Photoreactor (Batch /Continuous flow)	Determination of photocatalyst deactivation and quantification of photocatalyst lifetime	Description of the lifetime	Ref.
n-C_7H_{16}, SO_2	ZnO, TiO_2	Batch	Three hours was considered as a reactive period. The process was repeated until the concentration of n-C_7H_{16} (or SO_2) did not change. The total reactive times was referred to as lifetime. ZnO nearly lost all activity after 6 reactive periods (18 h) for degradation of n-C_7H_{16}. ZnO and TiO_2 both lost nearly all activity after 5 reactive periods(15 h) for degradation of SO_2.	15 h or 18 h	[28]
Toluene	TiO_2 P25	Continuous flow	As the reaction was progressed for 1200 min, C_{out}/C_{in} of toluene increase up to 0.7, this implies the photocatalyst was deactivated.	1200 min	[36]
Diethyl sulfide	Deposited TiO_2	Continuous flow	About 2.5 g of DES would be destroyed on 310 mg of photocatalyst before complete catalyst deactivation.	8.06 g DES/g TiO_2	[27]
Eosin B	CdS/HMS	Batch	The catalyst CdS/HMS after 1st run C/C_0 is 0, however in 3rd run, C/C_0 was ca. 1, which implies loss of activity.	3rd run	[41]
H_2S	TiO_2	Continuous flow	Under continuous flow mode, H_2S conversion dropped from 99.60 to 25.88% after 50 h of illumination, indicating a serious deactivation.	50 h	[35]

0 after the first run, and this value increased to ca. 1 after the third run, thereby revealing an activity loss. Jeong et al. [36]reported that the C_{out}/C_{in} of toluene increase up to 0.7, which implied that the photocatalyst was deactivated by reaction intermediates. Li et al. [35] reported a H_2S conversion drop from 99.60 to 25.88% after 50 h of illumination, thereby revealing a serious deactivation.

Quantification of the photocatalyst lifetime depends on the photoreactors type (i.e., batch or continuous-flow photoreactors).

Jing et al. [28] used a batch photoreactor and considered a reactive period of 3 h during the lifetime measurement process. The next reactive period began once the earlier reactive period was finished. The above process was repeated until constant concentration. The overall reaction time was referred to as lifetime. Yang et al. [41] also used a batch photoreactor with a C/C_0 of ca. 1 after the third run, thereby revealing that the photocatalyst lost its activity (i.e., the photocatalyst remained active for 3 runs).

Continuous-flow photoreactors are more suitable for quantifying photocatalyst lifetime by determining the reaction time. Jeong et al. [36] reported a photocatalyst lifetime of 1200min, while Li et al. [35] reported a photocatalyst lifetime of 50 h. Moreover, the mass of the target contaminants degraded by a unit mass of the photocatalyst can also be used to describe the photocatalyst lifetime. Vorontsov et al. [27] reported that ca. 2.5 g of DES were degraded by 310 mg of photocatalyst before complete photocatalyst deactivation, leading to a lifetime of 8.06 g DES/gTiO_2, which is more accurate and practical.

There is no unique definition for the unit of photocatalyst lifetime. The most exact definition is gDES/gTiO_2 in Vorontsov et al. [27] by using the continuous-flow photoreactors. Based on the limited literature, it is suggested to apply g target contaminant/g photocatalyst to characterize photocatalyst lifetime treating liquid contaminant.

4. Photocatalyst deactivation mechanisms

The main reasons behind photocatalyst deactivation recently reported are listed in Tables 4 and 5. According to Tables 4 and 5, the deactivation mechanisms are similar when treating gas and liquid pollutant. Catalyst deactivation is typically explained via reduction in the number of available surface active sites by strong surface adsorption of some intermediates and products formed during the photocatalytic degradation. Compare with the gas, the intermediates and products are more easily detached from the surface of the photocatalyst in the liquid phase. The intermediates leading to photocatalyst deactivation have been studied in detail. Cao et al. [54] reported that, during the degradation process of toluene, deactivation of TiO_2 catalysts was produced by the chemisorption of intermediates such as benzaldehyde and benzoic acid. Yang et al. [38] studied the degradation process of NO by Fourier transform infrared spectroscopy (FTIR) and showed that the nitrates attached to the photocatalysts were responsible for deactivation of TiO_2-rGO/ASC. Vorontsov et al. [27] studied the degradation of diethyl sulfide and identified sulfuric acid as the final surface product causing catalyst deactivation.

The reasons behind the deactivation of modified photocatalysts are not constrained to strong surface adsorption of some intermediates. Thus, Zhang and Yu [55] studied the degradation of acetone by Ag-TiO_2 and invoked aggregation

Table 4
Summary of the reasons of photocatalyst deactivation in gaseous phase

Target contaminant	Photocatalyst	Reason of photocatalyst deactivation	Ref.
n-C_7H_{16}, SO_2	ZnO, TiO_2	The deactivation mainly resulted from a semiconductor surface conduction change from N-type to P-type after the deactivation.	[28]
Toluene	TiO_2 P25	The adsorbed toluene produced deactivation, and the benzaldehyde generated mainly under low RH conditions by partial oxidation of toluene was the other cause of TiO_2 deactivation.	[36]
Diethyl sulfide	Deposited UV-100 TiO_2	Sulfuric acid was detected as the final surface product causing catalyst deactivation.	[27]
Toluene	TiBTiC	Deactivation of TiO_2 catalysts was produced by chemisorption of intermediates such as benzaldehyde and benzoic acid.	[54]
Acetylene	Deposited P25 Degussa TiO_2	Deactivation of catalyst was produced byadsorbed organic acids on the surface of the photocatalyst.	[37]
Toluene methylcyclohexane	TiO_2-ZnO thin film	Deactivation of catalyst was produced by the accumulation of highly stable partially oxidized compounds on the catalyst surface.	[33]
Acetone	Ag-TiO_2	The partially oxidized products not only accumulate on the surface of TiO_2, but also interact with Ag nanoparticles. Deactivation may also be caused by the aggregation of silver nanoparticles during the photocatalytic process.	[55]
H_2S	TiO_2	Catalyst poisoning was caused by the by-product S^0.	[35]
NO	Pt/TiO_2	Deactivation of TiO_2 catalysts was produced by the changes in the oxidation sates of Pt observed in the XPS scans over used samples.	[32]
NO	TiO_2-rGO	Deactivation of catalysts was produced by nitrates attaching on photocatalysts.	[38]
H_2S	TiO_2/M-MCM-41 (M = Cr or Ce)	Deactivation of catalysts was caused by the reduction of Cr^{6+} to $Cr^{3+}$and the blockage of active sites by sulfate accumulation on the surface.	[30]
Ambient office air in two office building locations in CT, USA	3 wt% WO_3 coated on Degussa P25	Deactivation of catalysts was produced byoxidable species that coated the photocatalyst surface.	[31]
Octamethyltrisiloxane	TiO_2 thin films	Deactivation of catalysts was produced by accumulation of hydroxylated SiO*x* on the TiO_2 surface.	[26]

Table 5
Summary of the reasons of photocatalyst deactivation in liquid phase

Target contaminant	Photocatalyst	Reason of photocatalyst deactivation	Ref.
Cyclohexane	H, H600, S450	Deactivation of Hombikat UV 100 (H) and Hombikatcalcined at 600°C (H600) was found to be irreversible owing to a high thermal stability of surface-adsorbed carbonates and carboxylates. For Solaronixnanopowder designed for coatings (S450), thermal stability of surface population was found to be significantly lower.	[42]
Phthalic acid	TiO_2 P25	Deactivation of catalyst was produced by surface adsorption of some carboxylic acid compounds reducing the number of available surface active sites. The deactivation of catalyst was not produced by pore blockage.	[44]
Four pharmaceutical micropollutants	TiO_2 thin films	Four pharmaceutical micropollutants were monitored in a biologically treated wastewater effluent. Deactivation of catalyst was produced by both effluent organic matter and inorganic constituents from wastewater effluent.	[45]
Organic dye	NMP-200 WACS-200	Deactivation of catalysts was produced by the deposition of the decomposed MO or the carbonaceous deposit.	[43]

of silver nanoparticles during the photocatalysis to explain the photocatalyst deactivation. Portela et al. [30]studied the degradation of $H_2SonTiO_2$/M-MCM-41 (M = Cr or Ce) and explained the catalytic deactivation by the reduction of Cr^{6+} to Cr^{3+}. Wu et al. [32] studied the degradation of NO on Pt/TiO_2 and observed changes in the oxidation sates of Pt of spent samples by X-ray photoelectron spectroscopy (XPS), which could result in the deactivation of Pt/TiO_2.

As indicated above, most of the research studies published focused on the single removal of various compounds. Carbonaro et al. [45] investigated the long-term performance of photocatalysts when dealing with more complex

matrices representative of contaminated water sources. The results indicated that effluent organic matter and inorganic constituents of these matrices contributed to the observed photocatalyst deactivation. Thus, the reasons behind deactivation are more complicated when using complex matrices as compared to single compounds.

The main reason of photocatalyst deactivation is the adsorption of intermediates, products and target pollutant onto the photocatalyst. However, deactivation of the modified photocatalyst may be due to the steady of the modifying. The deactivation mechanism is more complex when treating the real water and mixture. Under practical condition, the issue is more complex because non-target ingredient constitute the majority of dissolved solids and organic matter will act to scavenge a major fraction of reactive species generated by photocatalysts [45].

5. Regeneration of deactivated photocatalyst

Effective regeneration methods can overcome photocatalyst deactivation. The effectiveness of the regeneration methods was reviewed. For practical applications, the repeatability of the regeneration method is as important as its performance and should be emphasized.

5.1. Regeneration methods and efficiency

Deposition of some species was observed to produce photocatalyst deactivation, and a regeneration method using physical or chemical methods allowing the removal of such species have been considered. The main reported regeneration methods and their performance are listed in Table 6.

Miranda-García et al. [47] developed the concept of in-situ and ex-situ regeneration. For the in-situ regeneration treatments these authors used a fix bed system which was treated under a constant flow (0.45 L min^{-1}) of one of the following aqueous solutions: (i) 1 M H_2O_2 along with UV irradiation for 8 h; (ii) 3 MNaOH for 1 h; or (iii) 3 M NH_4OH for 1 h. For the ex-situ regeneration, the used photocatalysts was thermally treated in air at 400ºC for 180 min. The in-situ regeneration method does not required extracting the photocatalyst from the reactor and therefore is easier than the ex-situ regeneration method.

Four kinds of the regeneration methods (i.e., calcination, washing, oxidation, and adsorption) are studied herein.

5.1.1. Calcination

Calcination is one of the usual regeneration method of photocatalysts. It involves burning the intermediates absorbed on the photocatalyst surface and responsible for deactivation. An important point of calcination lies in finding the suitable temperature of the treatment.

Cao et al. [54] reported TiB to be only partially regenerated at 350ºC. In contrast, the activity of TiC was completely recovered after being regenerated at 420ºC. Temperature-programmed oxidation (TPO) was used to investigate the burning process of adsorbed carbon species on deactivated catalysts. As depicted in Fig. 6 [54], the TPO profile showed three peaks at 280, 360, and 420ºC, revealing that different carbon species were present on the deactivated catalyst. These results were in line with the regeneration tests revealing 420ºC as the temperature required to burn out all the adsorbed carbon species on the deactivated catalyst.

Kaewgun and Lee [43] studied the deactivation and regeneration of visible light-active brookite titania during the photocatalytic degradation of an organic dye. The deactivated photocatalysts were regenerated by calcination. Both NMP and nitrogen, responsible for the VLA properties in NMP-200 samples, were likely released by air calcination at temperatures above 250ºC for 2 h. Moreover, the surface area of the NMP samples calcined at temperatures above 350ºC rapidly decreased, and the average particle size increased with temperature because of sintering. Therefore, the NMP-200 samples were calcinated at either 200 or 250ºC in air. As expected, the deactivated photocatalyst was not completely be recovered after calcination at 200 and 250ºC. Thus, as shown in Fig. 7 [43], thermogravimetric analysis (TGA) revealed that the carbonaceous deposits on the used NMP-200 sample were only removed by combustion at temperatures above 420ºC.

Portela et al. [30] studied the photodegradation H_2S on TiO_2/M-MCM-41 (M = Cr or Ce) under UV-A and visible light. Deactivation was mainly caused by the reduction of Cr^{6+} to Cr^{3+} and the blockage of active sites via accumulation of sulfate on the catalyst surface. The deactivated catalyst was analyzed by thermogravimetry coupled with mass spectrometry (TG-MS). Since the sulfur species (SO and SO_2) were formed up to 460ºC, they can be also decomposed by calcination.

Excessive calcination temperatures may cause phase transformation (from anatase to rutile) and the sintering of nano-TiO_2. Therefore, some researchers regenerated their self-made photocatalysts at the same temperature used to prepare them [40,54]. Medina-Valtierra et al. [40] regenerated deactivated catalysts by burning out the chemisorbed carbon species in air at the preparation temperature (450ºC). For one regeneration cycle, the activity of the catalysts was almost completely recovered.

TPO and TGA analyses can be used to determine the calcination temperature. The effects of the calcination temperature on the photocatalyst surface should be also considered. The calcination regeneration method should not be used in the case of relative high temperatures are required to burn the pollutant from the photocatalyst surface. Thus, this treatment can seriously influence the characterization of the photocatalyst and reduce the photocatalytic activation.

5.1.2. Washing

Deactivated photocatalyst can be regenerated by washing with pure water, sonication, alkaline solutions, or organic solutions.

For selecting the washing method it is necessary to consider the characteristics of the pollutants adsorbed on the photocatalyst surface. Tuprakay and Liengcharernsit [39]studied the lifetime and regeneration of TiO_2during the removal of Cr(VI) from aqueous solution. The $Cr(OH)_3$ adsorbed on spent TiO_2 was leached upon treatment with NaOH solutions. A 3 M NaOH solution was suggested as a suitable reagent for regenerating TiO_2. Sun et al. [26] reported on the decomposition of gas-phase octamethyl-

Table 6
Summary of the main regeneration methods and their performance

Target contaminant	Photocatalyst	Regeneration method	Regeneration efficiency	Ref.
n-C_7H_{16}, SO_2	ZnO, TiO_2	Ultrasonically washing with deionized water and drying at 70°C for 24 h after centrifugation.	Deactivated ZnO or $TiO_2$was nearly regenerated to a full degree.	[28]
Cr(VI)	TiO_2	Used TiO_2 was adsorbed with $Cr(OH)_3$, washing off with a NaOH solution of varying concentration (0.01, 0.5, 1, and 3 M).	Washing off with 3 M NaOH was a suitable regeneration method.	[39]
Phthalic acid	TiO_2 P25	(I) Washing with solvent (0.1 g with 10 mL water followed by 10 mL methanol).	(I) The adsorbed species were not removed by washing, revealing strong interaction of the adsorbed compounds with the catalyst surface.	[44]
		(II) Treating with H_2O_2-30% H_2O_2, 10 mL for 1 g spent catalyst-solution for 1 h under stirring.	(II) The spent TiO_2 catalyst could be completely regenerated by treating with H_2O_2 solution.	
		(III) Thermal treatment at 350°C for 2 h in the presence of air.	(III) The heat treatment did not remove completely the adsorbed organic species from catalyst.	
Toluene	TiO_2 P25	Deactivated sample was exposed to UV light without toluene for 2000 min under 70% relative humidity condition.	Removal efficiency of toluene was completely recovered to the level on fresh photocatalyst.	[36]
Toluene	TiBTiC	At the preparation temperatures for TiB and TiC at 350 and 420°C respectively, both catalysts were regenerated in air for 2 h.	TiB was partially regenerated at 350°C. In contrast, the activity of TiC was completely recovered after being regenerated at 420°C in air.	[54]
Cyclohexane	H, H600, S450	Heat treatment in air at 400°C	Deactivation of Hombik at UV 100 (H) and Hombik at calcined at 600°C (H600) was found to be irreversibly deactivated.	[42]
			Solaronixnanopowder designed for coatings (S450) allowed regeneration by a heat treatment in air at 400°C.	
Methyl-orange	nano-ZnO	Ion exchange resin mixed bed (H/OH) was used to filtrate suspensions of nano-ZnO and methyl-orange after photocatalysis. The photocatalyst was regenerated during further backwash process.	Activity of nano-ZnO suspending solution photocatalyst was regenerated.	[56]
Toluene	TiO_2 coated on the inside of the cylinders.	(i) UV turn on + humidified air feeding. (ii) UV turn on + dried air feeding. (iii) UV turn off + dried air containing O_3 feeding. (iv) UV turn on + humidified N_2 gas feeding. (v) UV turn off + humidified air feeding.	(i) the conversion ratio returned to its original level (ii) high degree of regeneration (iii) introduced ozone effectively decomposed the intermediates over the TiO_2 catalyst. (iv) low degree of regeneration (v) low degree of regeneration	[57]
Diethyl sulfide	Deposited UV100	(i) Irradiation in humidified air	(i) Reactivation by irradiation in humidified air did not recover the activity completely.	[27]
		(ii) Irradiation with subsequent washing with water	(ii) The irradiation with subsequent washing with water provided complete reactivation.	
		(iii) Direct washing with water	(iii) Reactivation by direct washing with water completely recovered catalyst activity.	

(*Continued*)

Table 6 (*Continued*)

Acetylene	Deposited TiO_2	UV irradiation was kept constant but acetylene has been suppressed from the air stream. The UV irradiated reactor was swept by 500 mL/min of synthetic dry air during 6 h.	More than 80% of the adsorbed acids was mineralized into CO_2 by the photocatalytic regeneration.	[37]
Phenol	Deposited TiO_2	Regenerated in air for 3 h using the same temperature of preparation (450°C).	For one regeneration cycle, the activity of the catalysts was almost completely recovered. A slight decrease of the activity after two regeneration cycles was observed.	[40]
Organic dye	NMP-200 WACS-200	(i) NMP-200-VL#1 was washed with various solvents (i.e., methanol, (MeOH), ethanol (EtOH), isopropanol (IPA), or acetone). After washing, the titania particles were filtered and dried at 100°C for 4 h. (ii) Spent NMP-200 samples were heated at either 200 or 250°C in air.	(i) MeOH washing was shown to be the most effective approach (up to ~80% recovery of the fresh sample). (ii) NMP-200-VL#1 was not completely recovered by the recalcination at both 200°C and 250°C.	[43]
Octamethyltrisiloxane	TiO_2 thin films	Removal of the accumulated SiO*x* from the TiO_2 surface using dilute alkaline solutions without influencing the underlying TiO_2 film.	Treatment for 20 min in a NaOH solution with a pH higher than 12 was enough to complete remove the accumulated SiO*x*. The reactivity was comparable to that of a freshly prepared TiO_2 film.	[26]
Ammonia in petrochemical wastewater	TiO_2/LECA	Conducted following four-stage process: (i) washed with pour water, (ii) poured into a vessel which is equipped with an aeration system, (iii) remained in a 3 g/L sodium chloride solution for 3 h, (iv) heated at 250°C for 30 min.	The efficiency of the photocatalytic process after each reuse was ca. 14% less than efficiency of previous photocatalyst.	[46]
NO	TiO_2-rGO	Four different regeneration methods comprised of: (i) thermal regeneration, (ii) ultrasonic water rinse, (iii) ultrasonic ammonia rinse, and (iv) thermal vapor regeneration.	NO conversion ratios were 52.43–59.95, 63.72, and 62.23% after four different regeneration methods.	[38]
Eosin B	CdS/HMS-PDDA	The spent catalyst was placed in an air-isolated vessel. A stream of H_2S was produced by dropping HCl into Na_2S and filled into the vessel. Then the vessel was placed thermostatically at 100°C for 2 h.	CdS/HMS–PDDA was easily regenerated after the H_2S treatment, and the catalyst showed the same capability as the fresh sample even after 6 regenerations (accumulatively 151 runs).	[41]
H_2S	TiO_2	Irradiated by a 185 nm O_3 lamp for 48 h	The TiO_2 catalyst was successfully regenerated after a 48 h illumination process.	[35]
Selected emerging contaminants as Antipyrine and Atrazine et al.	Immobilized TiO_2	1 M H_2O_2 along with UV irradiation lasting 8 h. 3 M NaOH for 1 h. 3 M NH_4OH for 1 h. Thermally treated in air at 400°C for 180 min.	Calcination and H_2O_2/UV irradiation were the most efficient methods to recover the photocatalytic activity. Only the NH_4OH treatment seems to have a negative effect in the photocatalytic activity.	[47]

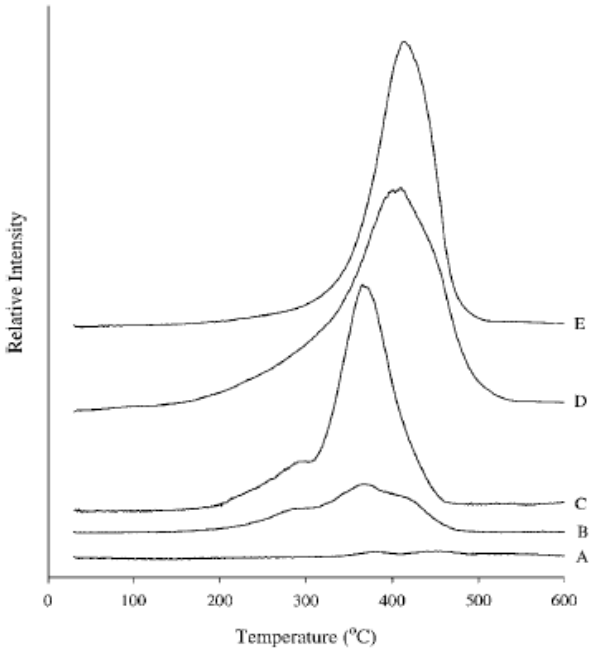

Fig. 6. Evolution of CO_2 during the temperature-programmed oxidation of carbon species on TiO_2 catalysts: (A) fresh TiB, (B) used TiA, (C) used TiPt, (D) used TiB, and (E) used TiC [54].

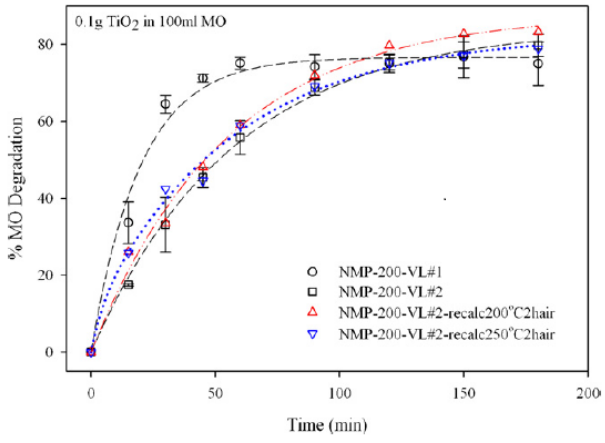

Fig. 7. The regeneration of NMP-200-VL#1, evaluated by the MO degradation under VL irradiation, by recalcination [43].

trisiloxane on TiO_2 thin film photocatalysts, which were deactivated by the accumulation of SiO*x*. A NaOH treatment (pH higher than 12) for 20 min was reported to be enough for the complete removal of the accumulated SiO*x*. The reactivity is the regenerated catalyst was comparable to that of afresh TiO_2 film.

During the washing regeneration process, the regeneration performance is different depending on the adsorbing strength of the pollutants on the photocatalyst surface. Vorontsov et al. [27] studied the reactivation of spent TiO_2 during the photocatalytic decomposition of gaseous diethyl sulfide. The results showed that reactivation by direct washing with water allowed to recover the activity completely. Gandhi et al. [44] studied the deactivation and regeneration of TiO_2 during the photocatalytic degradation of phthalic acid. A washing treatment with water and methanol was not effective in removing these adsorbed species from the surface of the spent catalyst, which indicated that the adsorbed species are strongly bonded to the surface

Sonicated washing is an effective regeneration method. Jing et al. [28] studied the degradation of n-C_7H_{16} and SO_2 on nano-ZnO and -TiO_2. A sonicated washing treatment with deionized water regenerated the spent photocatalyst almost completely. Sonication can also be carried out with a solvent. Thus, Yang et al. [38] studied the regeneration of activated semi-coke supported TiO_2-rGO nanocomposite photocatalysts during the removal NO under visible light. Among the four different regeneration methods tested, sonicated ammonia rinse was the optimum treatment and produced better results as compared to thermal regeneration, sonication by water rinse, and thermal vapor treatment.

Therefore, the adsorbed species should be considered when selecting the washing method. Combination of sonication and solvent washings is an effective method.

5.1.3. Oxidation

Photocatalyst can be regenerated by UV irradiation, oxidant treatment, and combination of both.

The UV irradiation method is easy to implement since it can be carried out in a photoreactor. Jeong et al. [36] studied a TiO_2 sample deactivated after photo-degradation of toluene. This sample was exposed to UV light without toluene for 2000 min under 70% relative humidity (RH) conditions. The partially reacted intermediates species present on TiO_2 were effectively oxidized to CO_2 under high RH conditions in the presence of UV light. Li et al. [35] successfully regenerated a catalyst deactivated during photocatalytic degradation of H_2S via a 48 h illumination treatment with a 185 nm O_3 lamp. Jeong et al. [57] compared the regeneration performance of five methods on a photocatalyst spent after photocatalytic degradation of gaseous toluene. The regeneration in a humid nitrogen stream with 254+185 nm irradiation was poor and similar to that obtained under a humid air stream without 254+185 nm irradiation. A dried air stream with 254+185 nm irradiation was effective in regenerating the catalyst. In addition, in the absence of UV irradiation, externally introduced ozone was effective in decomposing the intermediates adsorbed over the TiO_2 catalyst. A humid air and 254+185 nm irradiation treatment resulted in the conversion ratio returning to its initial value, and the TiO_2 surface restored its original color.

Oxidative treatments are usual oxidation method. Gandhi et al. [44] regenerated a catalyst spent during the degradation of phthalic acid by treating it with a 30% H_2O_2 solution (10 mL per 1 g of spent catalyst) for 1 h under stirring. The spent catalyst regenerated by the H_2O_2 treatment showed almost the same activity as the fresh catalyst. Jeong et al. [57] reported that ozone was effective in decomposing the intermediates adsorbed over a TiO_2 catalyst. The catalyst was used for the photocatalytic degradation of gaseous toluene using short-wavelength UV irradiation.

Oxidation treatments and UV irradiation are frequently combined to regenerate deactivated photocatalysts. Miranda-García et al. [47] studied four regeneration

approaches (i.e., 1 M H_2O_2 along with UV irradiation for 8 h, 3 M NaOH for 1 h, 3 M NH_4OH for 1 h, and a thermal treatment in air at 400ºC for 180 min) for photocatalysts used in the elimination of emerging contaminants in water. The H_2O_2/UV treatment was the most efficient regeneration strategy.

5.1.4 .Soft-mechanochemical ion exchange method

Li et al. [56] used a nano-ZnO photocatalyst for degrading methyl-orange. During the regeneration process, an ion exchange resin, the photocatalyst, and water were mixed evenly by airflow. The nano-ZnO photocatalyst and soluble carboxyl zinc species were gathered simultaneously upon the soft-mechanochemical process. Ionic intermediate products adsorbed on the photocatalyst and the surface hydroxyl ions present on the resin were exchanged as follows:

$$Zn(OH)HCO_3 + ROH \rightarrow Zn(OH)_2 + RHCO_3$$

$$Zn(OH)_2 \rightarrow ZnO + H_2O$$

The inorganic precipitated deposited on photocatalyst was removed by the following reaction:

$$CaCO_3 + 2ROH + 2RH \rightarrow R2Ca + 2RHCO_3$$

The dissoluble water Zn^{2+}were removed via the following ion exchange reaction:

$$Zn^{2+} + 2RH \rightarrow R2Zn + 2H^+$$

Byproducts and other inorganic ions were transferred into the resin phase. Thus, nano-ZnO photocatalyst were regenerated and reused.

Based on the above analysis and results, no matter the target pollutant is gas or liquid, the regeneration methods are basically calcination, washing, oxidation and so on. The calcination method requires to separate the photocatalyst from the rectors and appropriate temperature should be applied. Otherwise, it plays no role in the photocatalyst regeneration, if the temperate is too much low [54]. If the washing method can combine with the ultrasound, it will have a better effect. In addition, it is necessary to choose suitable cleaning agents, such as methanol, ethanol, NaOH, NH_4OH, and so on. It's easy to adopting the oxidation method in terms of UV irradiation or adding oxidant (e.g. O_3 and H_2O_2) into the photo-reactor. When treating gaseous pollutants, the regeneration effect is better under UV irradiation with inlet moist air or nitrogen, because abundant reactive OH radicals can be formed in the humid gas phase, accelerating the decomposition of the target pollutant [57]. During the degradation process of diethyl sulfide, Vorontsov et al. [27] found that high regeneration efficiency attributes to solubility of such products as acetaldehyde and SO_2 in water as well as lower rates of generation of products at high humidity. In addition, adding oxidant in UV irradiation is suitable for in-side regeneration. Furthermore, the in-side regeneration method is optimum for the practical application.

5.2. Multiple regeneration efficiency

Efficient regeneration methods should present high photocatalytic capabilities after multiple regeneration process. Yang et al. [38] studied the regeneration of activated semi-coke supported TiO_2-rGO nanocomposite photocatalysts used for the removal of NO under visible light. The effect of repetitive thermal vapor treatments on the regeneration efficiency was studied. The conversion of NO conversion decreased with the regeneration cycle up to the third regeneration cycle. It is worth noting that a TiO_2-rGO/ASC photocatalyst fabricated by a one-step solvothermal method exhibited an excellent stability.

Shavisi et al. [46] conducted a four-stage regeneration process on a photocatalyst deactivated during the degradation of ammonia in petrochemical wastewater. This process consisted of a pour waterwashing, an aeration washing, a 3 g L^{-1} sodium chloride solution remaining for 3 h, and a heating treatment at 250ºC for 30 min. The effect of the regeneration cycle on the regeneration efficiency was studied. The efficiency of the photocatalytic process decreased by ca. 14% after each reuse, revealing a poor regeneration efficiency for this regeneration method.

Therefore, the multiple regeneration efficiency is as important as the performance of a regeneration method. It is suggested to be well investigated in the same research of the photocatalyst application with the effective regeneration method.

6. Methods of prolonging the lifetime of photocatalyst

Apart from the regeneration of deactivated photocatalysts, modified photocatalysts are used to enhance the stability of photocatalysts, and this method is used to deal with deactivation. For example, Yang et al. [41] prepared acatalyst by coating a layer of poly(diallyl dimethylammonium) chloride (PDDA) on nanosized CdS pre-incorporated hexagonal mesoporous silica (HMS) sphere, and named it as CdS/HMS–PDDA. In contrast to the catalyst without PDDA-coating (CdS/HMS), which lost its activity after the third run, CdS/HMS–PDDA completely degraded organic pollutants for over 22 runs. The polyelectrolyte layer effectively prevented the cadmium species from leakage, and further delayed the photocorrosion of CdS via a back reaction using the photogenerated electrons remaining in CdS, this providing the catalyst with high stability and regeneratability. Fresno et al. [29] reported that good stability of a coupled TiO_2/SnO_2 and TiO_2/ZrO_2 photocatalyst during toluene PCO was mainly produced by an increased amount of accessible adsorbed water as a result of the presence of the second oxide. This higher amount of accessible water resulted in a higher capacity for the removal of adsorbed reaction intermediates.

Some experts improved the structure of photocatalytic reactors to prolong the lifetime of photocatalyst. Hay et al. [31] extended the lifetime of a photocatalytic-based air purifier in ambient air through the use of an adsorbent filter selected to capture large molecular weight compounds. Sannino et al. [34] studied the photocatalytic performance of $MoOx/TiO_2$ catalysts towards the selective oxidation of cyclohexane to benzene in a fixed bed reactor and in a

two-dimensional fluidized bed reactor. Unlike the fixed bed, catalyst deactivation was not observed in the fluidized bed reactor.

Methods of prolonging the lifetime of photocatalyst include the photocatalyst modification or the structure or functional improvement of photocatalyst reactor. Enhancing photocatalyst efficiency or increasing surface accessible water could be implemented for photocatalyst modification. This higher amount of accessible water resulted in a higher capacity for the removal of adsorbed reaction intermediates. On the other hand, the certain pretreatment could be supplied to capture large molecular weight compounds. The photo-reactor modification is easy to be implemented.

7. Characterization of the deactivated and regenerated photocatalysts

The characterization methods should be selected by the analyzing objectives for the deactivated and regenerated photocatalysts including XPS, FTIR, X-ray diffraction (XRD), GC-MS, high-performance liquid chromatography (HPLC), Brunauer–Emmett–Teller (BET), CHNO elemental analysis, diffuse reflectance infrared Fourier transform (DRIFT), TPO, and TGA, among others. The characterization methods used for the analysis of photocatalyst deactivation and regeneration are listed in Table 7.

Fresh, used, and regenerated photocatalysts were characterized by XPS, FTIR, GC-MS, HPLC, DRIFT, and CHNO

Table 7
Characterization methods for the analysis of photocatalyst deactivation and regeneration processes

Target contaminant	Photocatalyst	Characterization methods	Analyzing results	Ref.
Acetylene	Deposited P25 TiO_2	HPLC	For each extraction, three carboxylic acids have been identified and quantified: formic, oxalic and acetic acid. The most abundant organic acid extracted from the surface was formic acid. Beyond 4 h of treatment, the adsorbed amounts tend to reach a maximum, especially in the case of formic and acetic acids, suggesting that the carboxylic acid adsorption sites were close to saturation.	[37]
Phthalic acid	TiO_2 P25	BET	As no significant change was observed in the BET surface area of the washed spent catalyst in comparison to fresh catalyst, it was confirmed that the deactivation of the catalyst was produced via pore blocking by reactant or intermediate products of PCD.	[44]
		CHNO elemental analysis	The carbon content in the spent catalyst was 1.8 wt% and the washed spent catalyst contained 1.6 wt%, showing that some organic species were still in the spent catalyst. The thermal treatment reduced the carbon content from 1.6 to 0.5 wt.%, showing that some organic species was still present in the catalyst. CHNO elemental analysis of the spent catalyst regenerated by H_2O_2 treatment indicated nearly complete removal of organic species.	
		Zeta potential analysis	Fresh Degussa P25 TiO_2 catalyst was –20 mV, showing a negatively charged surface of the particles. The washed as well as thermally regenerated catalysts showed positive zeta potential (+32 mV and +25 mV). The H_2O_2 treated catalyst showed negative zeta potential value (–17 mV). The negatively charged surface in H_2O_2 treated catalyst showed similar characteristics than fresh TiO_2.	
		XRD	The XRD of spent catalyst after washing with water and methanol showed an additional broad peak in the 2θ range of 29–36°. Washing with water as well as methanol could not remove some adsorbed species formed during PCD from the catalyst surface. The phase composition and the crystallite size of the regenerated catalysts (thermal treatment and H_2O_2 treated) were compared with those of the fresh catalyst using XRD data and found to be unchanged. These results indicated that thermal or H_2O_2 treatments did not affect the structural properties of the catalyst.	
		FTIR	Catalyst deactivation was attributed to the presence of stable surface adsorbed organic species (phthalic acid or acid intermediates). Treatment of spent catalyst with H_2O_2 regenerates the catalyst by removing the adsorbed species.	

(*Continued*)

Table 7 (*Continued*)

Four pharmaceutical micropollutants.	TiO_2 thin films	XRD, XPS	No large changes in the bulk crystal structure or surface chemistry of the films were observed from XRD and XPS analyses, respectively.	[45]
		Profilometry analysis	TiO_2 films were exposed to a treated wastewater effluent matrix under treatment conditions for several days. Profilometry analysis revealed a slight increase in film thickness (1.84±0.61 μm), although the difference was not statistically significant.	
		SEM	SEM analysis revealed that the microcracks clearly visible in the virgin films were partially filled after the following exposure to treated wastewater effluent, and other debris began to appear on the surface of films.	
		EDS	EDS analysis indicated most of the surface debris was TiO_2, suggesting that some minor matrix-promoted deterioration of the film occurred.	
Toluene	TiO_2 P25	FTIR	The peaks centered at 1605 cm^{-1} and 1370 cm^{-1} can be attributed to aromatic ring vibration and CH_3 bending mode, implying the excess of non-decomposed toluene was adsorbed on surface of TiO_2 photocatalyst after reaction for 1000 min. The peaks observed at 1713 and 1230 cm^{-1} can be assigned to benzaldehyde, while the peaks located at 1691, 1313 and 1180 cm^{-1} were ascribed to benzoic acid, which are reaction intermediates.	[36]
		XPS	Major difference between bare and regenerated sample were observed in region of higher binding energies: the intensity of the shoulder at 531.5 eV corresponding to the OH species on TiO_2 increased drastically in intensity after regeneration.	
			Comparing C 1s spectrum of bare TiO_2 with that of the regenerated catalysts, the shoulder at high binding energies increased after each regeneration cycle, revealing the presence of carbon impurities on TiO_2 oxidized during regeneration step.	
n-C_7H_{16}, SO_2	ZnO, TiO_2	SPS	The deactivation mainly resulted from a semiconductor surface conduction change from N-type before the photocatalytic reaction to P-type after the deactivation. This deactivation was produced by semiconductor photocatalyst surface adsorbates revealed by SPS and XPS testing techniques as well as semiconductor chemical properties.	[28]
		XPS	XPS spectrum of S2p on the surface of TiO_2 nanoparticles after the deactivation, indicating that S element mainly existed as +6 according to the XPS analysis. SO_3 was the only oxidization product of SO_2. Thus, we concluded that the change of surface conduction type, and even deactivation, mainly resulted from the adsorption of SO_3.	
Toluene	TiSn TiZr TiO_2/SnO_2 TiO_2/ZrO_2	DRIFT	The DRIFT spectra of used $TiO_2$and TiZr revealed the presence of aromatic, carbonylic, and carboxylic compounds.	[29]
		GC-MS	In the analysis of a solid–liquid extract of the species adsorbed on the used TiO_2 catalyst, the main species found was benzoic acid, and peaks corresponding to benzyl alcohol and benzaldehyde, all of them formed by oxidation of the methyl group of toluene, were also observed by GC-MS analysis.	
Cyclohexane	H, H600, S450	TGA	The peak at 60 °C corresponded mostly to weakly adsorbed water, the second peak at higher temperatures at 200°C was assigned to water closer to the surface and associated with dehydroxylation. For the fresh materials, the weight loss at 60 °C was one order of magnitude higher for the H material, when compared to H600 and S450. For the spent catalysts, the weight loss at 60 °C decreased for all the materials, but less severely in the case of H600. The water desorption feature at Tr = 200°C clearly increased for S450, indicating an increase in the degree of hydration induced by the photocatalytic reaction.	[42]

(*Continued*)

Table 7 (*Continued*)

Diethyl sulfide	Deposited UV-100 TiO_2	SPME, GC-MS	Main surface products were diethyl disulfide, diethyl trisulfide, 1,2-bis(ethylthio)ethane, ethanesulfinic, ethanesulfonic acids, diethyl sulfoxide, diethyl sulfone, and sulfuric acid. Sulfuric acid was detected as the final surface product causing catalyst deactivation.	[27]
Toluene	TiATiBTiC	TPO	The curve for the TiA sample reveals three peaks at 280, 360, and 420°C, indicating that different carbon species were present on the deactivated catalyst. 420°C were needed to burn out all the adsorbed carbon species on the deactivated catalysts.	[54]
		FTIR	The deactivation of this type of catalyst arised from the irreversible adsorption of reaction intermediates such as benzaldehyde and benzoic acid. The complete removal of these strongly adsorbed intermediates required a burning temperature of ≥420°C.	
Selected emerging contaminants	Immobilized TiO_2	XPS	According to XPS results, fluoride, sulphur, and chloride adsorbed species can be removed from the catalysts surface by any treatment. Nevertheless, calcination was the most suitable process to remove nitrogen containing species.	[47]
H_2S	TiO_2	XPS	The XPS results showed that the catalyst activity changed with the different ratios of S^0 to S^{6+} (SO_4^{2-}) on the catalyst surface. The catalyst deactivated when the ratio of S^0 to SO_4^{2-} increased. However, this ratio continuously decreased during the continuous process of regeneration. With increasing amounts of SO_4^{2-} generated in the reaction, the yield of S^0 (catalyst poisoning) was inhibited.	[35]
NO	Pt/TiO_2	XPS	For Pt/TiO_2, changes in the oxidation sates of Pt were observed in the XPS scans of used samples, which could result in the deactivation of Pt/TiO_2.	[32]

elemental analysis with the aim to identify and quantify the species adsorbed on the photocatalyst and to analyze the deactivation and regeneration mechanisms.

BET, scanning electron microscopy (SEM), and profilometry analyses were used to identify the textural properties of a photocatalyst deactivated during the degradation of phthalic acid. Gandhi et al. [44] reported that the regeneration of a spent catalyst by thermal and H_2O_2 treatments did not affect the textural properties and the BET surface area of the regenerated catalyst to a large extent. Carbonaro et al. [45] exposed TiO_2 films to a wastewater effluent matrix under treatment conditions for several days. Profilometry analysis revealed a slight increase in film thickness (1.84±0.61 μm), although the difference was not statistically significant.

TPO was used to investigate the burning process of adsorbed carbon species on deactivated catalysts. Duringthe degradation of toluene by TiA, TiB and TiC catalysts, Cao et al. [54] found a TPO profile for spent TiA with three peaks at 280, 360, and 420°C. These results indicated that different carbon species were present on the deactivated catalyst. The temperature of 420°C was required to burn out all the adsorbed carbon species on the deactivated catalysts.

The analyzing methods should be selected by the analyzing objectives for the deactivated and regenerated photocatalyst, in order to clarify the deactivation mechanism and regeneration performance.

8. Conclusions

Spent TiO_2 catalysts showed lower catalytic activity than fresh photocatalyst, thereby revealing deactivation. Photocatalyst deactivation has been found largely limit the practical applications of photocatalysis. Deactivation and regeneration studies on photocatalysts needs to be studied in detail to enable practical application of this technique.

In this review, we summarized the experimental conditions of recent investigations on deactivation and regeneration of photocatalysts. We found that most of the studies were carried out under idealized conditions using experimental systems. These systems do not allow easy simulation of more practical engineered treatment operations. Therefore, real wastewater or ambient air as target contaminants should be used in future experiments by using continuous-flow photoreactors.

Deactivation is produced via strong surface adsorption of some intermediates and products formed during the photocatalytic degradation process. When single compounds are degraded in complex matrices such as treated wastewater effluents, the deactivation process becomes more complex. Deactivation of doped photocatalysts may be produced by aggregation or reduction/oxidation of the doped element.

We tried to summarize various regeneration methods and their regeneration efficiency. In situ regeneration is suitable for practical engineered treatment operations. Multiple efficient regeneration methods should still possess high photocatalytic efficiencies such that the performance of the photocatalyst can be maintained after each regeneration process. Studies of prolonging the lifetime of photocatalystshould be carried out based on the regeneration methods in future studies.

Acknowledgments

This work was supported by the National Science Foundation of China (51208172, 51508383 and 51508384), the Fundamental Research Funds for the Central Universities (2017B10414), the Research Fund of the Tianjin Key Laboratory of Aquatic Science and Technology (No. TJKLAST-ZD-2017-03) and the Key Technology R&D Program of Henan Province of China (172102210096).

References

[1] G. Del Moro, A. Mancini, G. Mascolo, C. Di Iaconi, Comparison of UV/H_2O_2 based AOP as an end treatment or integrated with biological degradation for treating landfill leachates, Chem. Eng. J., 218 (2013) 133–137.

[2] Q.N. Liao, F. Ji, J.C. Li, X. Zhan, Z.H. Hu, Decomposition and mineralization of sulfaquinoxaline sodium during UV/H_2O_2 oxidation processes, Chem. Eng. J., 284 (2016) 494–502.

[3] R.C.H.M. Hofman-Caris, D.J.H. Harmsen, L. Puijker, K.A. Baken, B.A. Wols, E.F. Beerendonk, L.L.M. Keltjens, Influence of process conditions and water quality on the formation of mutagenic byproducts in UV/H_2O_2 processes, Water Res., 74 (2015) 191–202.

[4] S. Bahnmüller, C.H. Loi, K.L. Linge, U.V. Gunten, S. Canonica, Degradation rates of benzotriazoles and benzothiazoles under UV-C irradiation and the advanced oxidation process UV/H_2O_2, Water Res., 74 (2015) 143–154.

[5] T. Coenen, W. Van de Moortel, F. Logist, J. Luyten, J.F.M. Van Impe, J. Degrève, Modeling and geometry optimization of photochemical reactors: Single- and multi-lamp reactors for UV-H_2O_2 AOP systems, Chem. Eng. J., 96 (2013) 174–189.

[6] L. Prieto-Rodríguez, I. Oller, N. Klamerth, A. Agüera, E.M. Rodríguez, S. Malato, Application of solar AOPs and ozonation for elimination of micropollutants in municipal wastewater treatment plant effluents, Water Res., 47 (2013) 1521–1528.

[7] J. Vittenet, W. Aboussaoud, J. Mendret, J.-S. Pic, H. Debellefontaine, N. Lesage, K. Faucher, M.-H. Manero, F. Thibault-Starzyk, H. Leclerc, A. Galarneau, S. Brosillon, Catalytic ozonation with γ-Al_2O_3 to enhance the degradation of refractory organics in water, Appl. Catal. A: Gen., 504 (2015) 519–532.

[8] F. Qi, W. Chu, B. Xu, Ozonation of phenacetin in associated with a magnetic catalyst $CuFe_2O_4$: The reaction and transformation, Chem. Eng. J., 262 (2015) 552–562.

[9] P. Van Aken, R. Van den Broeck, J. Degrève, R. Dewil, A pilot-scale coupling of ozonation and biodegradation of 2,4-dichlorophenol-containing wastewater: The effect of biomass acclimation towards chlorophenol and intermediate ozonation products, J. Clean. Prod., 161 (2017) 1432–1441.

[10] J. Nawrocki, B. Kasprzyk-Hordern, The efficiency and mechanisms of catalytic ozonation, Appl. Catal. B: Environ., 99 (2010) 27–42.

[11] Y. Nie, L. Zhang, Y.Y. Li, C. Hu, Enhanced Fenton-like degradation of refractory organic compounds by surface complex formation of $LaFeO_3$ and H_2O_2, J. Hazard. Mater., 294 (2015) 195–200.

[12] M. Aleksić, H. Kušić, N. Koprivanac, D. Leszczynska, A.L. Božić, Heterogeneous Fenton type processes for the degradation of organic dye pollutant in water - The application of zeolite assisted AOPs, Desalination, 257 (2010) 22–29.

[13] P. Oancea, V. Meltzer, Photo-Fenton process for the degradation of Tartrazine (E102) in aqueous medium, J. Taiwan Inst. Chem. Eng., 44 (2013) 990–994.

[14] P. Yongrui, Z. Zheng, M. Bao, Y. Li, Y. Zhou, G. Sang, Treatment of partially hydrolyzed polyacrylamide wastewater by combined Fenton oxidation and anaerobic biological processes, Chem. Eng. J., 273 (2015) 1–6.

[15] Y. Ren, Y. Yuan, B. Lai, Y. Zhou, J. Wang, Treatment of reverse osmosis (RO) concentrate by the combined Fe/Cu/air and Fenton process (1stFe/Cu/air-Fenton-2ndFe/Cu/air), J. Hazard. Mater., 302 (2016) 36–44.

[16] J. Hartmann, P. Bartels, U. Mau, M. Witter, W.v. Tümpling, J. Hofmann, E. Nietzschmann, Degradation of the drug diclofenac in water by sonolysis in presence of catalysts, Chemosphere, 70 (2008) 453–461.

[17] D.K. Kim, K.E. O'Shea, W.J. Cooper, Mechanistic considerations for the degradation of methyl tert-butyl ether (MTBE) by sonolysis: Effect of argon vs. oxygen saturated solutions, Ultrason. Sonochem., 19 (2012) 959–968.

[18] M.S. Saghafinia, S.M. Emadian, M. Vossoughi, Performances evaluation of Photo-Fenton process and Sonolysis for the treatment of Penicillin G formulation effluent, Procedia Environ. Sci., 8 (2011) 202–208.

[19] M. Lee, J. Oh, Sonolysis of trichloroethylene and carbon tetrachloride in aqueous solution, Ultrason. Sonochem., 17 (2010) 207–212.

[20] N.N. Mahamuni, Y.G. Adewuyi, Advanced oxidation processes (AOPs) involving ultrasound for waste water treatment: A review with emphasis on cost estimation, Ultrason. Sonochem., 17 (2010) 990–1003.

[21] K. Ji, H. Dai, J. Deng, H. Zang, H. Arandiyan, S. Xie, H. Yang, 3DOM $BiVO_4$ supported silver bromide and noble metals: High-performance photocatalysts for the visible-light-driven degradation of 4-chlorophenol, Appl. Catal. B: Environ., 168–169 (2015) 274–282.

[22] J.C. Ahern, R. Fairchild, J.S. Thomas, J. Carr, H.H. Patterson, Characterization of BiOX compounds as photocatalysts for the degradation of pharmaceuticals in water, Appl. Catal. B: Environ., 179 (2015) 229–238.

[23] R. Jaiswal, N. Patel, A. Dashora, R. Fernandes, M. Yadav, R. Edla, R.S. Varma, D.C. Kothari, B.L. Ahuja, A. Miotello, Efficient Co-B-codoped TiO_2 photocatalyst for degradation of organic water pollutant under visible light, Appl. Catal. B: Environ., 183 (2016) 242–253.

[24] Y.P. Luo, J. Chen, J.W. Liu, Y. Shao, X.F. Li, D.Z. Li, Hydroxide $SrSn(OH)_6$: A new photocatalyst for degradation of benzene and rhodamine B, Appl. Catal. B: Environ., 182 (2016) 533–540.

[25] H. Park, Y. Park, W. Kim, W. Choi, Surface modification of TiO_2 photocatalyst for environmental applications, J. Photochem. Photobiol. C: Photochem. Rev., 15 (2013) 1–20.

[26] R.D. Sun, A. Nakajima, T. Watanabe, K. Hashimoto, Decomposition of gas-phase octamethyltrisiloxane on TiO_2 thin film photocatalysts - Catalytic activity, deactivation, and regeneration, J. Photochem. Photobiol. A: Chem., 154 (2003) 203–209.

[27] A.V. Vorontsov, E.N. Savinov, C. Lion, P.G. Smirniotis, TiO_2 reactivation in photocatalytic destruction of gaseous diethyl sulfide in a coil reactor, Appl. Catal. B: Environ., 44 (2003) 25–40.

[28] L.Q. Jing, B.F. Xin, F.L. Yuan, B.Q. Wang, K.Y. Shi, W.M. Cai, H.Q. Fu, Deactivation and regeneration of ZnO and TiO_2 nanoparticles in the gas phase photocatalytic oxidation of n-C_7H_{16} or SO_2, Appl. Catal. A: Gen., 275 (2004) 49–54.

[29] F. Fresno, M.D. Hernández-Alonso, D. Tudela, J.M. Coronado, J. Soria, Photocatalytic degradation of toluene over doped and coupled (Ti,M)O_2 (M=Sn or Zr) nanocrystalline oxides: Influence of the heteroatom distribution on deactivation, Appl. Catal. B: Environ., 84 (2008) 598–606.

[30] R. Portela, M.C. Canela, B. Sánchez, F.C. Marques, A.M. Stumbo, R.F. Tessinari, J.M. Coronado, S. Suárez, H2S photodegradation by TiO_2/M-MCM-41 (M = Cr or Ce): Deactivation and by-product generation under UV-A and visible light, Appl. Catal. B: Environ., 84 (2008) 643–650.

[31] S.O. Hay, T.N. Obee, C. Thibaud-Erkey, The deactivation of photocatalytic based air purifiers by ambient siloxanes, Appl. Catal. B: Environ., 99 (2010) 435–441.

[32] Z. Wu, Z. Sheng, Y. Liu, H. Wang, J. Mo, Deactivation mechanism of PtOx/TiO_2 photocatalyst towards the oxidation of NO in gas phase, J. Hazard. Mater., 185 (2011) 1053–1058.

[33] M.D. Hernández-Alonso, I. Tejedor-Tejedor, J.M. Coronado, M.A. Anderson, Operando FTIR study of the photocatalytic oxidation of methylcyclohexane and toluene in air over TiO_2-ZrO_2 thin films: Influence of the aromaticity of the target molecule on deactivation, Appl. Catal. B: Environ., 101 (2011) 283–293.

[34] D. Sannino, V. Vaiano, P. Ciambelli, P. Eloy, E.M. Gaigneaux, Avoiding the deactivation of sulphated MoO_x/TiO_2 catalysts in the photocatalytic cyclohexane oxidative dehydrogenation by a fluidized bed photoreactor, Appl. Catal. A: Gen., 394 (2011) 71–78.
[35] X. Li, G.Q. Zhang, H.G. Pan, Experimental study on ozone photolytic and photocatalytic degradation of H_2S using continuous flow mode, J. Hazard. Mater., 199–200 (2012) 255–261.
[36] M.G. Jeong, E.J. Park, H.O. Seo, K.D. Kim, Y.D. Kim, D.C. Lim, Humidity effect on photocatalytic activity of TiO_2 and regeneration of deactivated photocatalysts, Appl. Surf. Sci., 271 (2013) 164–170.
[37] F. Thevenet, C. Guillard, A. Rousseau, Acetylene photocatalytic oxidation using continuous flow reactor: Gas phase and adsorbed phase investigation, assessment of the photocatalyst deactivation, Chem. Eng. J., 244 (2014) 50–58.
[38] W.W. Yang, C.H. Li, L. Wang, S.N. Sun, X. Yan, Solvothermal fabrication of activated semi-coke supported TiO_2-rGO nanocomposite photocatalysts and application for NO removal under visible light, Appl. Surf. Sci., 353 (2015) 307–316.
[39] S. Tuprakay, W. Liengcharernsit, Lifetime and regeneration of immobilized titania for photocatalytic removal of aqueous hexavalent chromium, J. Hazard. Mater., 124 (2005) 53–58.
[40] J. Medina-Valtierra, J. García-Servín, C. Frausto-Reyes, S. Calixto, The photocatalytic application and regeneration of anatase thin films with embedded commercial TiO_2 particles deposited on glass microrods, Appl. Surf. Sci., 252 (2006) 3600–3608.
[41] Y.H. Yang, N. Ren, Y.H. Zhang, Y. Tang, Nanosized cadmium sulfide in polyelectrolyte protected mesoporous sphere: A stable and regeneratable photocatalyst for visible-light-induced removal of organic pollutants, J. Photochem. Photobiol. A: Chem., 201 (2009) 111–120.
[42] J.T. Carneiro, J.A. Moulijn, G. Mul, Photocatalytic oxidation of cyclohexane by titanium dioxide: Catalyst deactivation and regeneration, J. Catal., 273 (2010) 199–210.
[43] S. Kaewgun, B.I. Lee, Deactivation and regeneration of visible light active brookite titania in photocatalytic degradation of organic dye, J. Photochem. Photobiol. A: Chem., 210 (2010) 162–167.
[44] V.G. Gandhi, M.K. Mishra, P.A. Joshi, A study on deactivation and regeneration of titanium dioxide during photocatalytic degradation of phthalic acid, J. Ind. Eng. Chem., 18 (2012) 1902–1907.
[45] S. Carbonaro, M.N. Sugihara, T.J. Strathmann, Continuous-flow photocatalytic treatment of pharmaceutical micropollutants: Activity, inhibition, and deactivation of TiO_2 photocatalysts in wastewater effluent, Appl. Catal. B: Environ., 129 (2013) 1–12.
[46] Y. Shavisi, S. Sharifnia, M. Zendehzaban, M.L. Mirghavami, S. Kakehazar, Application of solar light for degradation of ammonia in petrochemical wastewater by a floating TiO_2/LECA photocatalyst, J. Ind. Eng. Chem., 20 (2014) 2806–2813.
[47] N. Miranda-García, S. Suárez, M.I. Maldonado, S. Malato, B. Sánchez, Regeneration approaches for TiO_2 immobilized photocatalyst used in the elimination of emerging contaminants in water, Catal. Today, 230 (2014) 27–34.
[48] X. Yan, X. Xu, J. Liu, R. Bao, L. Li, Regeneration of photocatalysts by in situ UV irradiation in photocatalytic membrane reactor, Russ. J. Appl. Chem., 89 (2016) 94–98.
[49] C. Han, M.Q. Yang, B. Weng, Y.J. Xu, Improving the photocatalytic activity and anti-photocorrosion of semiconductor ZnO by coupling with versatile carbon, Phys. Chem. Chem. Phys., 16 (2014) 16891–16903.
[50] N. Zhang, M.Q. Yang, S. Liu, Y. Sun, Y.J. Xu, Waltzing with the versatile platform of graphene to synthesize composite photocatalysts, Chem. Rev., 115 (2015) 10307–10377.
[51] M.Q. Yang, C. Han, N. Zhang, Y.J. Xu, Precursor chemistry matters in boosting photoredox activity of graphene/semiconductor composites, Nanoscale, 7 (2015) 18062–18070.
[52] B. Weng, M.Q. Yang, N. Zhang, Y.J. Xu, Toward the enhanced photoactivity and photostability of ZnO nanospheres via intimate surface coating with reduced graphene oxide, J. Mater. Chem. A, 2 (2014) 9380–9389.
[53] K.Q. Lu, L. Yuan, X. Xin, Y.J. Xu, Hybridization of graphene oxide with commercial graphene for constructing 3D metal-free aerogel with enhanced photocatalysis, Appl. Catal. B: Environ., 226 (2018) 16–22.
[54] L.X. Cao, Z. Gao, S.L. Suib, T.N. Obee, S.O. Hay, J.D. Freihaut, Photocatalytic oxidation of toluene on nanoscale TiO_2 catalysts: studies of deactivation and regeneration, J. Catal., 196 (2000) 253–261.
[55] L. Zhang, J.C. Yu, A simple approach to reactivate silver-coated titanium dioxide photocatalyst, Catal. Commun., 6 (2005) 684–687.
[56] Y. Li, Z. Jiao, N. Yang, H. Gao, Regeneration of nano-ZnO photocatalyst by the means of soft-mechanochemical ion exchange method, J. Environ. Sci., 21 (2009) S69–S72.
[57] J. Jeong, K. Sekiguchi, K. Sakamoto, Photochemical and photocatalytic degradation of gaseous toluene using short-wavelength UV irradiation with TiO_2 catalyst: Comparison of three UV sources, Chemosphere, 57 (2004) 663–671.